



## Porosity Verification of Gas-Bearing F3 Reservoir, Al Wafa Oil Field, Ghadames Basin, Libya

BAHIA MUFTAH BEN GHAWAR<sup>1</sup>, IBRAHIM R. IBRAHIM<sup>2</sup>, QUSAI A. EL-MUQASSBI<sup>1</sup>, and SALEM M. AL-GHELLALI<sup>1</sup>

<sup>1</sup>Geological Engineering Department, Engineering Collage, University of Tripoli, Tripoli, Libya

<sup>2</sup>Department of Geophysics, Faculty of Science, University of Libya, Tripoli, Libya

Corresponding author: B.Ben-Ghawar@uot.edu.ly

Manuscript received: March, 21, 2025; revised: August, 15, 2025;

approved: October, 21, 2025; available online: March, 30, 2026

**Abstract** - Porosity estimation of gas reservoir rocks is a crucial challenge for many oil fields, which may drive to the uncertainty of reserve assessment. However, wirelines are normally available, and considered a neat source of porosity measurement, where logs and core samples are two sources of direct and indirect rock porosity data. The main objective of this paper is to demonstrate the impact of the porosity logs on the water saturation ( $S_w$ ) assessment of the gas-bearing F3 sandstone reservoir (Aouinet Uennin Formation, Devonian). This geologic formation represents a giant reservoir of the Al Wafa Gas and Oil Field, Ghadames Basin (Libya). The studied reservoir (Devonian) is a clean gas-bearing sandstone reservoir that has a shale content of less than 25 %, which may be considered a potassium feldspar sandstone rock type. Besides, different log categories of the porosity - total porosity ( $\Phi_{nd}$ ), neutron porosity ( $\Phi_n$ ), and sonic porosity ( $\Phi_s$ ) illustrate high values of the water saturation ( $S_w$ ) estimation due to the gas appearance. Whereas the density porosity ( $\Phi_d$ ) yields the lowest values of the  $S_w$ . Moreover, the  $\Phi_d$  demonstrates a high agreement with the core porosity ( $\Phi_{core}$ ), which verifies less uncertainty of the petrophysical assessment in the F3 Sandstone gas-bearing reservoir.

**Keywords:** petrophysical properties, Aouinet Uennin Formation, well logging, sandstone

© IJOG - 2026

### How to cite this article:

Ghawar, B.M.B., Ibrahim, I.R., El-Muqassbi, Q.A., and Al-Ghellali, S.M., 2026. Porosity Verification of Gas-Bearing F3 Reservoir, Al Wafa Oil Field, Ghadames Basin, Libya. *Indonesian Journal on Geoscience*, 13 (1), p.77-87. DOI:10.17014/ijog.12.3.77-87

## INTRODUCTION

### Background

Any petrophysical and geological studies of reservoir rock is concerned with quantities and quality evaluation of reservoir characteristic and productivity. However, porosity is a main physical property that dominates a high enhancing contribution of oil and gas fields recovery, which in turn provides a suitable solving well production ques-

tion. Thus, petrophysical assessment assumes all available subsurface data within the oil fields, that gives a useful indicator and understanding impact of the depositional environment and lithofacies changes on the reservoir characteristics. Generally, the porosity ( $\Phi$ ) is essential input property for computing reserve estimation as saturation of fluid type; water saturation ( $S_w$ ) or hydrocarbon saturation ( $S_h$ ), as well as to build a static and dynamic petrophysical models. This petrophysical assess-

ment is a useful tool required on the judgement of the reservoir strategic development plan. However, the porosity ( $\Phi$ ) could be estimated in a laboratory, by measuring the available core samples or from well logs. Hence, nuclear and acoustic logs have commonly been utilized for the porosity evaluation. Neutron porosity ( $\Phi_n$ ), litho-density (bulk density,  $\rho_b$ ), and interval travel time ( $\Delta T$ ) are measured logs that provide the porosity of subsurface rocks. These logs are influenced by the fluid type filling of the bore holes, as well as the pore space or lithofacies type (Asquith and Gibson 1982b). Thus, the  $\Phi_n$  log records dramatically low porosity values of gas bearing formation pores (Serra *et al.*, 1980). Whereas the interval travel time ( $\Delta T$ ) log is affected by the gas, while the bulk density ( $\rho_b$ ) has less effect with the hydrocarbon (gas).

Many published petrophysical studies apply suitable porosity values of gas bearing and/or oil reservoir rocks. Quintero and Bassiouni (1998) proposed a new model to estimate the porosity of gas-bearing rocks depending on both bulk density and the neutron logs, which were recorded from a near detector. Also, they introduced a set of parameters (gas density, drilling fluid saturation, and salinity) within this new model. While Osman *et al.* (2021) have utilized density porosity to evaluate Kharita Formation (Cretaceous gas reservoir), Western Desert, Egypt. Whereas Wang *et al.* (2022) have applied a complex reservoir analysis (CRA) technique based on the well logs data, in order to define accurate tight gas reservoir lithology and porosity. On the other hand, Minh *et al.* (2001) have preferred to employ a confident procedure by integrating nuclear magnetic resonance (NMR) and sonic porosity, instead of the neutron and density porosity logs, for gas bearing formation. However, the Al-Wafa Oil Field is a giant gas and oil reservoir rock (Echikh, 1998) in the northwest Ghadames Basin, Libya, where this site was produced from Aouniet-Ouenine Formation (Middle - Upper Devonian). Most studies have been focused to realize sedimentology parameter, and to build a geological and petrophysical models for economic hydrocarbon potential of the F3 reservoir (Hlal, 2022; Fello and Turner, 2004). Thus,

integration between geophysical, geological, and petrophysical data of the F3 sandstone reservoir was conducted to illustrate the reservoir quality (Soltan and Hrouda, 2022). On the other hand, two petrophysical evaluations have documented the sandstone part of the Aouniet-Ouenine Formation (F3) which were based on core and log data of well A37-NC169a (Basal *et al.*, 2023; Basal *et al.*, 2024). Whereas Khalifa and Morad (2015) have illustrated the effect of the middle Devonian reservoir quality on the combined petrographic and geochemical data, which delineate facies distribution and diagenetic processes. Accordingly, all the previous petrophysical studies of the F3 Sandstone reservoir (Aouinet Uennin Formation) (Figure 1c) have utilized the neutron porosity as the porosity log and did not take into consideration the gas effect. Therefore, the present work tried to shed some light on the fluctuation of the logs porosity values (neutron, density, and interval travel time) due to gas effects, in addition a suitable porosity log uses reservoir saturation as an essential petrophysical assessment. Thus, measured core porosity results were utilized to verify the calculated porosity of the gas bearing F3 Sandstone. This porosity investigation is required if an advanced tool or core samples are not available, such as the NMR logs. Further, this work will allow more accuracy of the 3D building petrophysical models.

### Geological/Stratigraphical Settings

Sirt, Murzaq, Kufra, Ghadames Basins and Cyrenaica Platform are all major structural provinces of Libya (Figure 1), where they directly related to the tectonic history of Libya and all tectonic events of the world (Conant and Goudarzi, 1967; Klitzsch, 1968; Bellini and Massa, 1980; Mikbel, 1979). Generally, the geological history of Libya was formed from Precambrian to Cenozoic Era (Hallett and Clark-Lowes 2016). The Ghadames Basin is one of western sedimentary basins that has an extend into Algeria and Tunisia, which is a large and deep depression known as Illizi Basin in Alegria. Structurally, Ghadames Basin is characterized by fault-bounded structural highs surrounding a central depression. The main

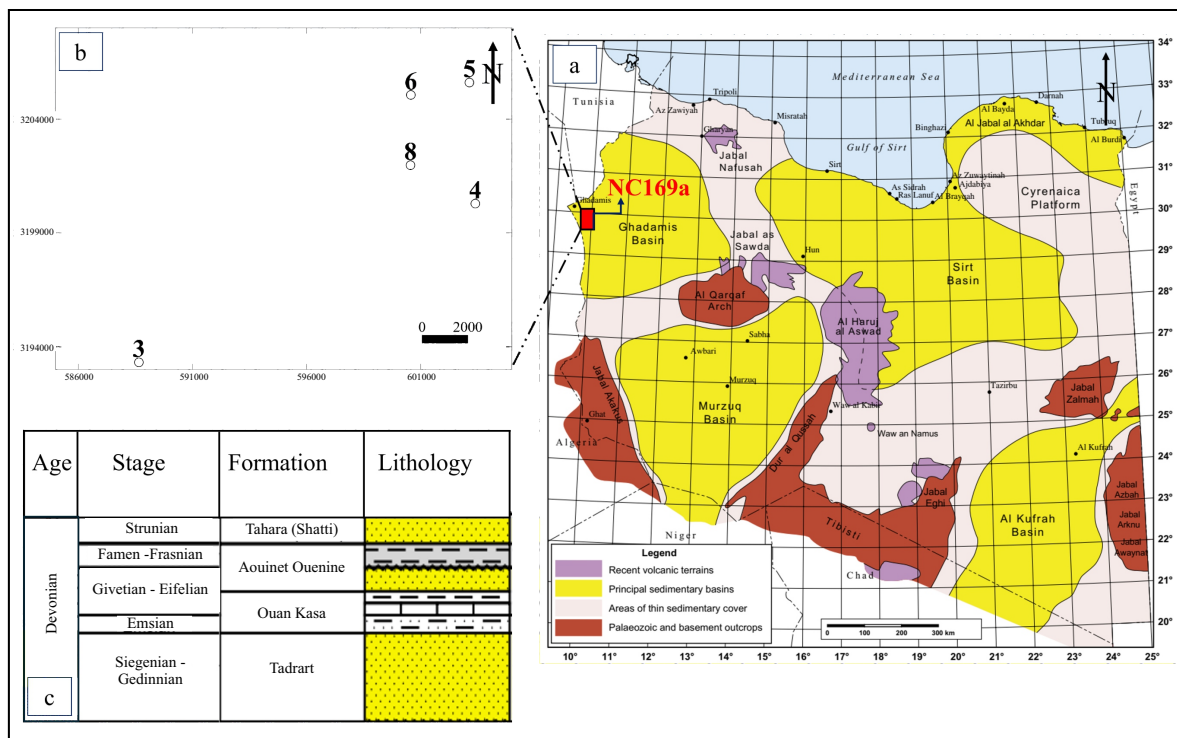


Figure 1. a. Major sedimentary basins of Libya (after Hallett and Clark-Lowes, 2016), b. Location of the studied wells from Al Wafa Field-NC 169a, and c. Sequence stratigraphy of the Devonian age (after Hallett and Clark-Lowes, 2016).

tectonic boundary elements of the basin are the Dahra-Nafusah High (Talemzane Arch) to the north, the Qarqaf Uplift and the Huggar Shield to the south, the Amguid- El Biod High to the west, and the western flank of the younger Sirt Basin to the east. Paleozoic is a dominant stratigraphic sequence of the Ghadames Basin that underlain a thin Mesozoic - Tertiary section (Hammuda, 1980). The Palaeozoic section is composed of a sequence of alternating sandstones and mudstones with occasional interbedded carbonate beds. However, the term Aouniet-Ouenine was first introduced by Lelubre (1946), and was named after a drilled borehole in the western part of Jabal Gargaf in Fezzan (southern Libya). However, the term Aouniet-Ouenine Group was first used by Massa and Moreau-Benoit (1976), and is generally characterized by an alternation of shale, siltstone and sandstone (Figure 2). In addition, early studies consider the Aouniet-Ouenine Formation is a group, which compresses four formations based on fauna (Couvinian to Famenian) (Bellini and Massa, 1980). However, five wells have been selected from Al Wafa Oil Field,

which belongs to the Concession 169a, southwest of the Ghadames Basin (Figure 1b).

### METHODS AND MATERIALS

Well logging is one of the universal subsurface tools that provides valuable information in the petroleum industry. These tools measure natural nuclear or electrical characteristics of subsequent rocks, as physical properties that are in turn considered petrophysical properties. Thus, porosity and fluid saturation are conventional petrophysical properties that could be estimated based on the well logs or core samples. So, nuclear, electrical, and acoustic are three different principal log tool categories that have been running within most wells of the studied area. Therefore, these recorded logs were collected from five wells (3, 4, 5, 6, and 8) of the F3 Sandstone reservoir (Aouniet-Ouenine Formation). It worth mentioning that the gamma ray (GR), spectral gamma ray (NGS), neutron ( $\Phi_n$ ), litho-density ( $\rho_b$  and PEF) are the nuclear logs. Whereas deep resistivity ( $R_d$ ) is an electrical log,

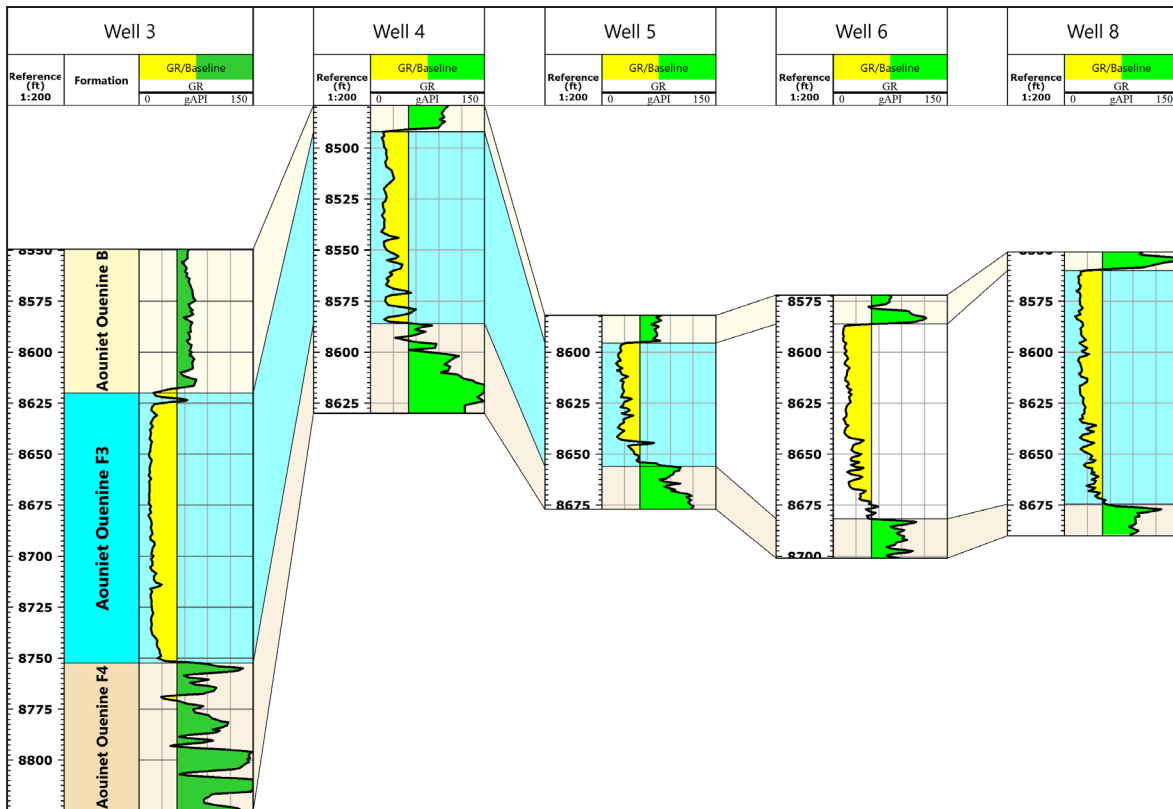


Figure 2. F3 Sandstone (Aouinet Uennin Formation) boundary delineation by gamma ray logs of the studied wells, Al Wafa oil field - Ghadames Basin, Libya.

and the interval travel time ( $\Delta T$ ) are acoustic logs. Thus, processing and application of these logs are helpful to compute the essential petrophysical properties of the F3 Sandstone: volume of shale ( $V_{sh}$ ), porosity ( $\Phi$ ), water saturation distribution ( $S_w$ ).

Generally, the GR and PEF logs are mainly lithology logs, and the  $\Phi_n$ ,  $\rho_b$ , and  $\Delta T$  are porosity indicators that are also useful to define the lithology, used together (a combination between them). While the NGS logs are clay mineral discrimination type based on standard cross plots (Bateman, 1985). Therefore, the volume of shale ( $V_{sh}$ ) is a result of the GR logs processing by Equations 1 and 2 (Asquith and Gibson, 1982a), which is required for effective porosity ( $\Phi_e$ ) computation.

$$IGR = \frac{GR_{log} - GR_{clean}}{GR_s - GR_{clean}} \dots\dots\dots (1)$$

Where:  
 IGR is Gamma ray index (fraction),  
 GR log is Gamma ray log reading (API),

GR<sub>clean</sub> is minimum log reading (API), and  
 GR<sub>sh</sub> is the maximum log reading (API).

$$V_{sh} = 0.33 \times [(2^{2 \times IGR}) - 1] \dots\dots\dots (2)$$

Where:  
 $V_{sh}$  is volume of shale (fraction).

The nuclear ( $\Phi_n$  and  $\rho_b$ ) and acoustic ( $\Delta T$ ) logs have commonly been utilized for the porosity evaluation as mentioned above. Moreover, the quantitative porosity of the reservoir rocks could be read directly from the neutron porosity ( $\Phi_n$ ) log, or by processing both bulk density ( $\rho_b$ ) and interval travel time ( $\Delta T$ ) logs. These logs have a distinctive principal operation which is dependent on fluid types filling of the pore space or lithofacies type (Asquith and Gibson, 1982b). The neutron porosity log ( $\Phi_n$ ) is commonly used to measure the porosity of subsurface open or cased holes, as a measure of hydrogen content in the subsurface rocks. It worth mentioning,

that the neutron log ( $\Phi_n$ ) is very sensitive to the presence of gas bearing rocks as previously explained. Generally, the total porosity ( $\Phi_t$  or  $\Phi_{nd}$ ) is the average between the  $\Phi_n$  and density porosity ( $\Phi_d$ ), while an effective porosity ( $\Phi_e$ ) is the  $\Phi_t$  eliminated of the shale content ( $V_{sh}$ ). Thus, Equations 3, 4, and 5 are applied to compute the porosities of the F3 Sandstone reservoir, which depends on lithology, pore space, and  $V_{sh}$  content. Whereas Wyllie *et al.* (1958) have used Equation 6 that has been employed to calculate the sonic porosity ( $\Phi_s$ ) from the interval travel time ( $\Delta T$ ) logs. This sonic porosity result is corrected for gas effect if it is multiplied by 0.7 as per Hilchie empirical correlation (1978) (Asquith and Gibson, 1982b). Accordingly, results of the porosity estimation of the F3 Sandstone reservoir will be compared with the available measured core porosity values of the studied wells (3, 4, and 5). Therefore, the studied porosity will be evaluated by different procedures to notify the gas effect on reservoir saturation assessment. The first procedure combined both the  $\Phi_n$  and  $\Phi_d$  (Equation 4), while the second procedure is applied the Hilchie correlation. Whereas, the third is considered with the  $\Phi_d$  as the total porosity of the F3 Sandstone reservoir (Equation 3):

$$\Phi_d = \frac{\rho_{bma} - \rho_b \log}{\rho_{bma} - \rho_f} \dots\dots\dots (3)$$

Where:  
 $\Phi_d$  is density porosity (fraction),  
 $\rho_b$  is bulk density (gm/cc),  
 $\rho_f$  is fluid density, g/cc, and  
 $\rho_{bma}$  is apparent matrix density (g/cc).

$$\Phi_{nd} = \sqrt{\frac{(\Phi_n^2) + (\Phi_d^2)}{2}} \dots\dots\dots (4)$$

Where:  
 $\Phi_{nd}$  = neutron-density porosity (fraction),  
 $\Phi_n$  is neutron porosity (fraction), and  
 $\Phi_d$  is density porosity (fraction).

$$\Phi_e = \Phi_x (1 - V_{sh}) \dots\dots\dots (5)$$

Where:  
 $\Phi_e$  is effective porosity (fraction).

$$\Phi_s = \frac{(\Delta T \log - \Delta T_{ma})}{(\Delta T_f - \Delta T_{ma})} \dots\dots\dots (6)$$

Where:  
 $\Phi_s$  is sonic porosity (fraction),  
 $\Delta T \log$  is interval travel time log reading ( $\mu\text{sec}/\text{ft}$ ),  
 $\Delta T_{ma}$  is apparent matrix interval time ( $\mu\text{sec}/\text{ft}$ ), and  
 $\Delta T_f$  is fluid interval time,  $\mu\text{sec}/\text{ft}$ .

Reserve evaluation of oil fields defines the hydrocarbon quantity that could be produced, which is a function of a water saturation ( $S_w$ ) percent. Thus, several formulas were applied to assess the  $S_w$  (Rahuma and Ghawar, 2019), and Archie Equation (7) as one of these formulas used in the present work. This equation is dependent on the Archie parameters; cementation factor ( $m$ ), saturation exponent ( $n$ ), and Tortuosity Factor ( $a$ ). The parameters ( $a$ ,  $m$ , and  $n$ ) could be extracted from special core analysis, which is not available. Whereas, formation water resistivity ( $R_w$ ) is another required parameter of the Archie formula. So, Resistivity of NaCl Water Solutions (Schlumberger, 2009), Pickett technique (Pickett, 1973) are conventional techniques that provide the  $R_w$  value of reservoir rocks. Hence, variety of the water saturation results is responding to Formation Factor ( $FF = a/\Phi^m$ ) and the resistivity data (Ghawar and Rahuma, 2017). However, an arithmetic average (Equation 8) was used to manifest the petrophysical properties of the F3 Sandstone reservoir.

$$S_w = \sqrt{\frac{axR_w}{\Phi^m x R_t}} \dots\dots\dots (7)$$

Where:  
 $S_w$  is water saturation (fraction),

Rt is deep formation resistivity (Rd, Ohm.m),  
 m, n, a are Archie parameters,  
 Rw is formation water Resistivity (Ohm.m), and  
 Φ is porosity.

$$X_{average} = \frac{\sum_{i=1}^n (X_i \times X_{hi})}{\dots\dots\dots} \dots\dots\dots (8)$$

Where:

X<sub>average</sub> is arithmetic average reservoir property (fraction),  
 X is reservoir property (fraction), and  
 h is thickness of each depth (feet).

**RESULT AND DISCUSSION**

The gamma ray (GR) logs have allowed distinctive features of clastic rock sequences, and boundary delineation (Ghawar *et al.*, 2025). Thus, the measured GR log of the studied wells allow picking out of the F3 Sandstone reservoir rock boundary. Figure 2 displays the correlation of the F3 Sandstone as a low GR log reading among wells, presented as a clean rock interval, with an increasing the GR

log at lower parts. Thus, tidally influenced littoral bars are depositional environment of the F3 Sandstone (Chaouchi *et al.*, 1997). In addition, based on the shape of GR logs, the studied F3 Sandstone reveals a prograding sedimentary sequence system of the Aouniet-Ouenine Formation (Serra and Abbott, 1982). Further, it defines the lithology for the petrophysical assessment that determines the bulk density (ρb) and neutron porosity (Φn) on the standard lithology chart (Figure 3). This chart demonstrates three compressed main lithofacies lines; where the green line represent sandstone, blue line for limestone, and the rose line is for the dolomite. The plotting points are grouped close to the sandstone line, which symbolizes the volume of shale (Vsh) of less than 25 %, as the Vsh colour scale bar illustration. The average of the volume of shale (Vsh) values of the Aouniet-Ouenine F3 and cross-thickness es are summarized in Table 1. Also, all the points above the sandstone line (green colour) reveal gas content within the F3 Sandstone (Asquith and Gibson, 1982a). Further, Serra and Serra (2003) have documented the potassium feldspar sandstone, as appears on the attached plotting along the sandstone line with a high potassium (K, %), and a low thorium (Th, ppm) concentration.

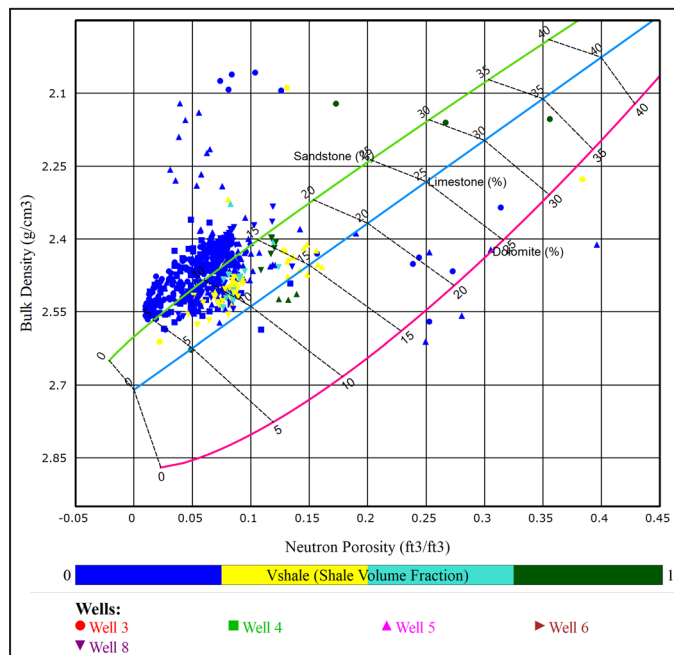


Figure 3. Bulk density versus neutron porosity between the studied wells, F3 Sandstone reservoir (Aouniet-Ouenine Formation).

Table 1. Thickness And The Average Volume of Shale (Vsh), Logs Porosity ( $\Phi_n$ ,  $\Phi_d$ ,  $\Phi_{nd}$ , and  $\Phi_s$ ) of The F3 Sandstone Reservoir (Aouniet-Ouenine Formation) of The Studied Wells

Wells	3	4	5	6	8
h, ft	130	94	60.5	95.5	114.5
Vsh, %	6.32	15.43	14.96	17.39	21.03
$\Phi_n$ (%)	4.99	5.45	9.31	5.36	7.44
$\Phi_d$ (%)	10.70	10.17	12.48	13.14	10.73
$\Phi_{nd}$ (%)	8.57	8.29	11.48	10.06	9.30
$\Phi_s$ (%)	3.47	-	-	6.00	4.40
$\Phi_{core}$ (%)	9.75	9.58	18.76	-	4.40

Meanwhile, the standard charts between thorium (Th, ppm) and potassium (K, %) concentration cross plots are applied to disclose the clay minerals groups that are combined within the F3 Sandstone (Aouniet-Ouenine reservoir). This plot reveals illite, (mixed layer clay), chloride, and montmorillonite that are the clay mineral group, which were recognized in wells 3, 4, 5, and 6 within the studied F3 reservoir. While kaolinite and heavy thorium bearing minerals were in well 8 as displayed on Figure 4. Also, these clay mineral groups have been disclosed in the Middle Devonian sandstone that Khalifa and Morad (2015) explained them as diagenetic alteration processes.

However, the bulk density and neutron porosity cross plot emphasizes the GR log correlations of the clean sandstone. This yields an apparent matrix density ( $\rho_{ma}$ ), and interval travel time ( $\Delta T_{ma}$ ) equal to 2.65 g/cc and 55.5  $\mu\text{sec}/\text{ft}$ , respectively. These  $\rho_{ma}$  and  $\Delta T_{ma}$  values were used in the density porosity ( $\Phi_d$ ) and sonic porosity ( $\Phi_s$ ) calculation. In general, the average porosity of the log porosity and core results do not exceed 15 % and not less than 5 % as demonstrated in Table 1 and Figures 3 and 5. Accordingly, all the results of the porosity logs ( $\Phi_n$ ,  $\Phi_d$ ,  $\Phi_{nd}$ , and  $\Phi_s$ ) in the studied wells were correlated with the available core porosity of wells (3, 4, and 5) as displayed on Figure 5. The comparison between the log and core porosity provides validation process of the porosity evaluation of the gas bearing F3 Sandstone. Furthermore, the  $\rho_b$  and  $\Phi_n$  logs overlay a quick and significant technique of the gas detected (Figure 6). This Figure clearly shows the presence of the gas; through the whole depth intervals section of the F3 Sandstone reservoir which is occupied with the gas. Hence, the separation magnitude between two logs reflects the amount of gas content filling the pore space. Thus, the gas content increase

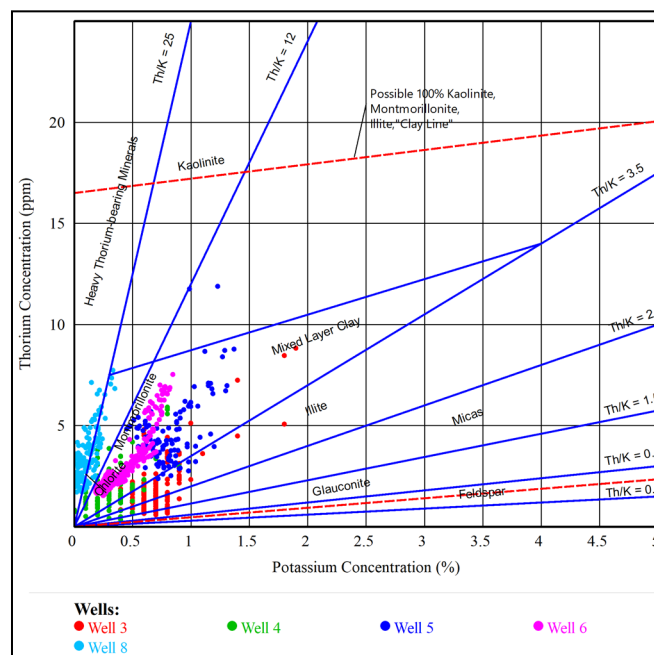


Figure 4. Thorium (Th) and potassium (K) concentration cross plot of the studied wells, F3 Sandstone reservoir (Aouniet-Ouenine Formation).

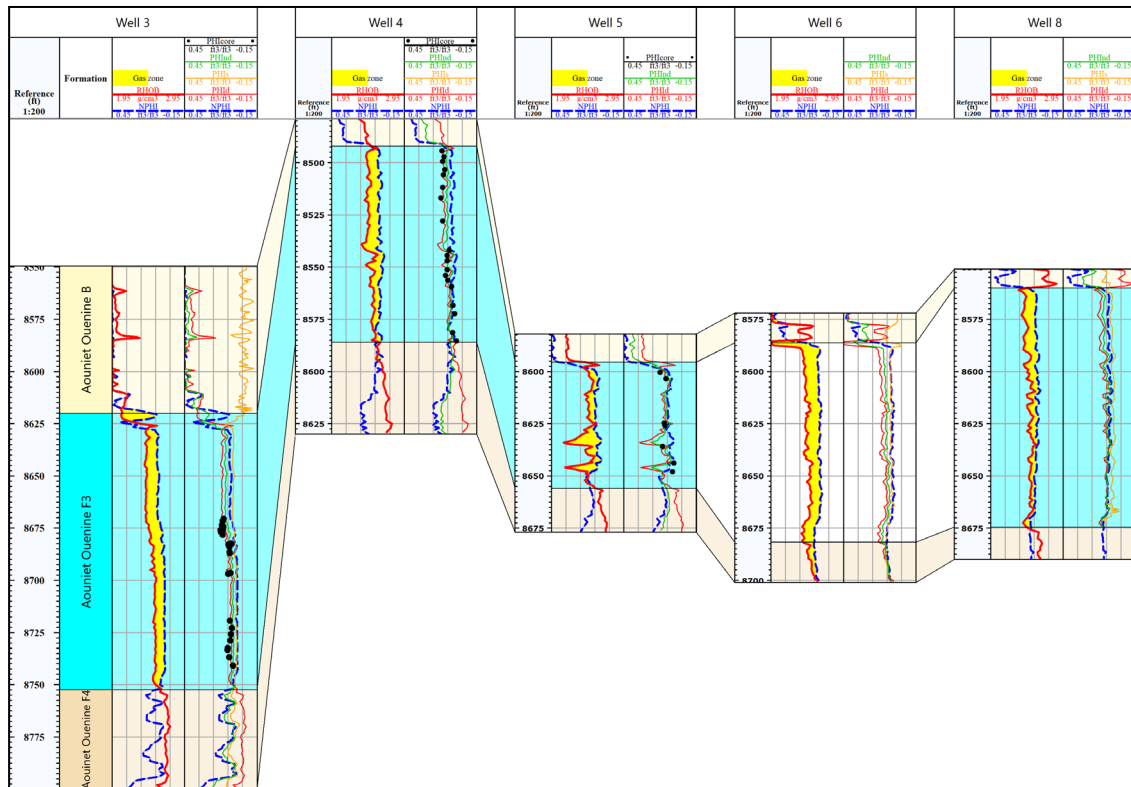


Figure 5. Gas detection zone by the neutron porosity ( $\Phi_n$ ) and bulk density ( $\rho_b$ ) a correlation among the studied wells of the F3 Sandstone reservoir (Aouniet-Ouenine Formation).

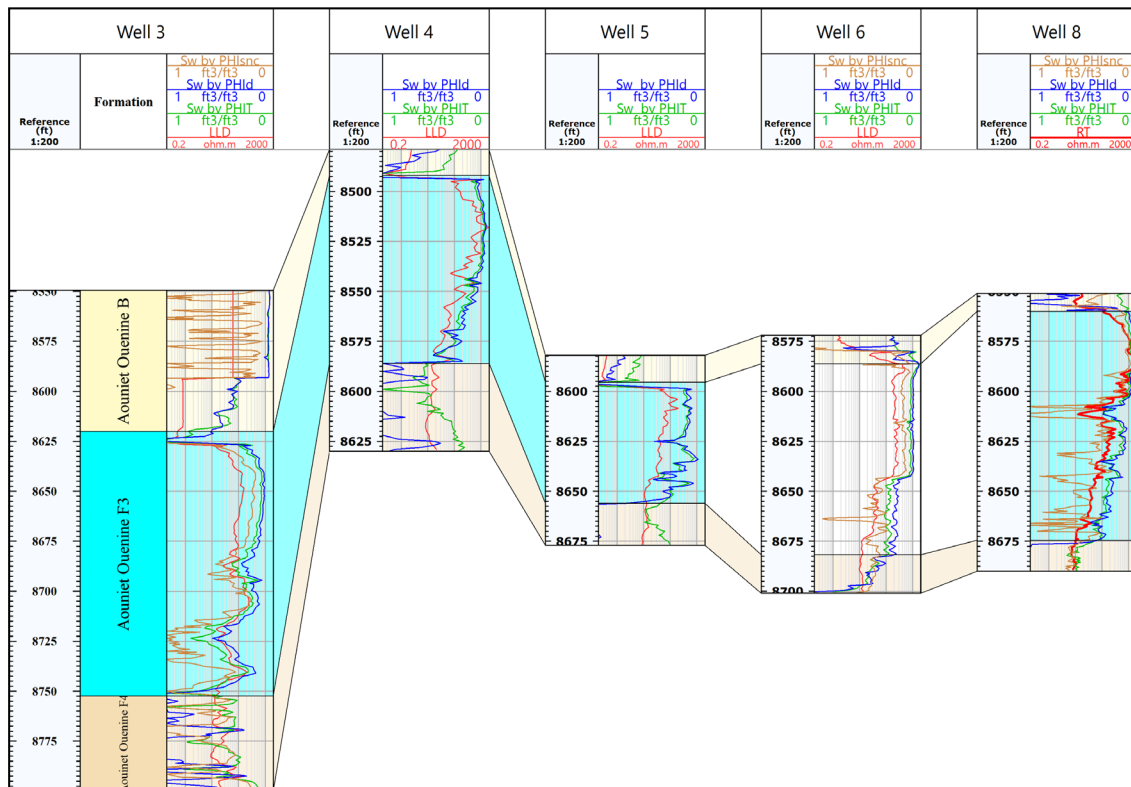


Figure 6. Comparison between the water saturation ( $S_w$ ) that has resulted in different log porosity of each studied well and the deep resistivity ( $R_d$ ) logs of the F3 Sandstone reservoir (Aouniet-Ouenine Formation).

leads to a separation increase and the attribute decrease of the  $\Phi_{nd}$  and  $\Phi_n$  results. On the other hand, the  $\Phi_d$  illustrates less affected by the gas issue within the studied wells, as well as highly confirmed with the core porosity. Furthermore, the Hilchie formula of sonic porosity ( $\Phi_s$ ) exposes a similar reduction behaviour of the  $\Phi_{nd}$  and  $\Phi_n$  where avsimilar conclusion has been observed by Miah (2014). Correspondingly, the  $\Phi_d$  is more acceptable than the  $\Phi_{nd}$ ,  $\Phi_n$ , and  $\Phi_s$  in the petrophysical assessment.

As mentioned above, the Archie formula is applied to estimate the water saturation, and a fundamental hydrocarbon reserve evaluation of the reservoir rocks. This formula is dependent on the porosity, resistivity, and Archie parameters. The formation water resistivity ( $R_w$ ) is defined by using standard resistivity of NaCl Water Solutions (Schlumberger, 2009), which is equal to 0.02 Ohm. m. Whereas, the porosity gives an estimation of a storage capacity, while the effective porosity is an important part of a productivity or a flow capacity. Thus, estimation of the water saturation ( $S_w$ ) of the F3 Sandstone reservoir has taken in consideration by different calculated log porosity results ( $\Phi_{nd}$ ,  $\Phi_d$ , and  $\Phi_s$ ) that verify an impact of the  $\Phi$  property on the petrophysical evaluation of studied gas bearing reservoir. It worth mentioning that, the interval travel time ( $\Delta T$ ) logs are not recorded of the wells (4 and 5). Hence, Figure 6 illustrates a comparison between the water saturation ( $S_w$ ) that has resulted in different log porosity of each studied well and the measured deep resistivity logs ( $R_d$ ). In general, the average water saturation is not exceeding 50 % among the studied wells as shown on Figure 7. This result is confirmed with Basal *et al.* (2023). Moreover, the calculated water saturation by density porosity ( $\Phi_d$ ) demonstrates lower results of the F3 Sandstone reservoir than the total ( $\Phi_{nd}$ ) and sonic ( $\Phi_s$ ) in the studied wells, respectively. Furthermore, the gradual changes in the interval travel time ( $\Delta T$ ) logs, attributed to the presence of gas, lead to an overestimation of porosity, which subsequently results in a higher percentage of  $S_w$  values (Asquith and Krygowski, 2004).

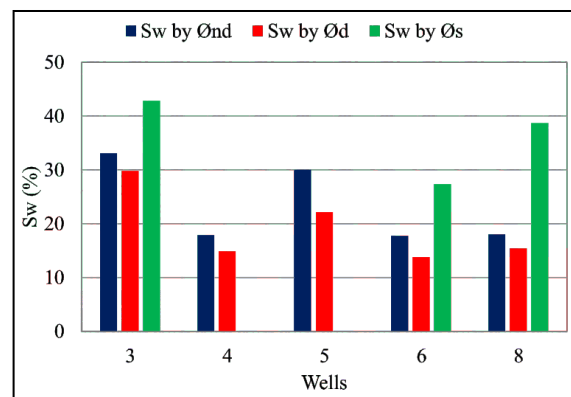


Figure 7. Comparison of the average water saturation estimation by using different porosity logs.

## CONCLUSIONS

Porosity ( $\Phi$ ) is a physical property that has numerous contributions of reservoir studies, such as rock type and reservoir modeling. Hence, the total porosity ( $\Phi_{nd}$ ), neutron porosity ( $\Phi_n$ ), density porosity ( $\Phi_d$ ), and sonic porosity ( $\Phi_s$ ) are the main parameters derived from three logs, which may be susceptible subject to corrections due to hydrocarbon and shale effects. However, the Devonian F3 reservoir (Aouinet Uennin Formation) is considered a clean sandstone, which has less than 25 % of the shale volume ( $V_{sh}$ ). This sandstone rock contains a lower content of the thorium (Th) mineral compared with the potassium (K) mineral (may be a potassium feldspar sandstone rock type). Also, the main clay mineral groups recognized in the studied F3 reservoir are illite, mixed-layer clay, chloride, and montmorillonite within wells 3, 4, 5, and 6. While the kaolinite and heavy thorium-bearing minerals are in well 8.

Reduction of the neutron - density porosity, neutron porosity, and sonic porosity of the F3 Sandstone reservoir due to the gas effect caused uncertainty of the water saturation as the petrophysical evaluation. Therefore, the measured core porosity ( $\Phi_{core}$ ) emphasizes the utility of the density porosity ( $\Phi_d$ ) rather than the neutron and sonic porosity logs.

Porosity logs demonstrate an alteration of the water saturation ( $S_w$ ), where the sonic porosity ( $\Phi_s$ ) provides higher values of average water satu-

ration rather than the neutron - density ( $\Phi_{nd}$ ) and density porosity ( $\Phi_d$ ). Therefore, the  $\Phi_d$  provides the lowest average water saturation.

#### ACKNOWLEDGMENTS

The authors thank the administration of The Mel-litah Oil & Gas B. V company, Libyan Branch, for providing the requested data.

#### REFERENCES

- Asquith, G.B. and Gibson, C.R., 1982a. *Basic Relationships of Well Log Interpretation: Chapter I*, p.1-5.
- Asquith, G.B. and Gibson, C.R., 1982b. *Porosity Logs: Chapter IV*, p.66-68.
- Asquith, G.B. and Krygowski, D., 2004. *Basic Well Log Analysis*. edited by G. Asquith, D. Krygowski, S. Henderson, and N. Hurley. Tulsa, Oklahoma: American Association of Petroleum Geologists.
- Basal, A.M.K., Sarhan, M.A., Alfarog, M.G., and El Bahrawy, A., 2023. Relative Permeabilities as Dynamic Petrophysical Parameters, Wafa Field, Ghadamis Basin, North West Libya. *Scientific Journal for Damietta Faculty of Science*, 13 (3), p.47-52.
- Basal, A.M.K., Mohammad A.S., Alfarog, M.G., and Ahmed, E., 2024. Geophysical Modeling and Reservoir Performance of Aouinet Wanin F3B Sandstone in Well A37 NC 169A, Wafa Field, Ghadamis Basin, Libya. *Arabian Journal of Geosciences*, 17 (12), 325. DOI: 10.1007/s12517-024-12131-y.
- Bateman, R.M. 1985. *Openhole Log Analysis and Formation Analysis*. United States.
- Bellini, E. and Massa, D., 1980. A Stratigraphic Contribution to the Palaeozoic of the Southern Basins of Libya. p.3-56. *In: Salem, M.J. and Busrewil, M.T. (eds.) Second Symposium on the Geology of Libya, 1*. London: Academic Press.
- Chaouchi, R., Malla, M.S., and Kichou, F., 1997. Sedimentological Evolution of the F3 Sandy Bar of the Western Alrar Field (Eifelian-Givetian), Illizi Basin, Algeria. *Bulletin Du Service Géologique de l'Algérie*, 8, p55-70.
- Conant, L.C. and Goudarzi, G.H., 1967. Stratigraphic and Tectonic Framework of Libya1. *AAPG Bulletin*, 51 (5), p.719-730. DOI: 10.1306/5D25C0C9-16C1-11D7-8645000102C1865D.
- Echikh, K., 1998. *Geology and Hydrocarbon Occurrences in the Ghadamis Basin, Algeria, Tunisia, Libya*. Geological Society, London, *Special Publications*, 132 (1), p.109-129.
- Fello, N.M. and Turner, B.R., 2004. Depositional Environments of the Upper Ordovician Mamuniyat Formation, NW Murzuq Basin, Libya , *Proceedings of 3<sup>rd</sup> International Symposium on Geophysics, Tanta*, p.166-182.
- Ghawar, B.M.B. and Rahuma, K.M., 2017. Variety of Cementation Factor between Dolomite and Quartzite Reservoir. *University Bulletin*, 2 (19), p151-162.
- Ghawar, B.M., Fathi, M.S., Al-Jawadi, A.S., and Yaseen S.S., 2025. Rock Physics Application for Shaly Sand Evaluation: A Case Study for Lower Nubian Sandstone Reservoir, Eastern Sirte Basin, Libya. *Journal of Applied Geophysics*, 241,105813. DOI: 10.1016/j.jappgeo.2025.105813.
- Hallett, D. and Clark-Lowes, D., 2016. *Petroleum Geology of Libya: Second Edition*. Amsterdam: Elsevier, 404p.
- Hammuda, O.S., 1980. Geologic Factors Controlling Fluid Trapping and Anomalous Freshwater Occurrence in the Tadrart Sandstone, Al Hamadah Al Hamra' area, Ghadamis Basin, p.501-508. *In: Salem, M.J. and Busrewil M.T. (eds.), Academic Press. London: Second Symposium on Libya, Geology of Libya*.
- Hlal, O.A.R., 2022. Delineate of Middle Devonian Aouinet Ouenine F3 Sand by Using Petrophysical and Sedimentological Analysis in South Wafa Field, Ghadamis Basin, Libya. *The Mediterranean and North African Conference and Exhibition (MEDINA)*.
- Khalifa, M.A. and Morad, S., 2015. Impact of Depositional Facies on the Distribution

- of Diagenetic Alterations in the Devonian Shoreface Sandstone Reservoirs, Southern Ghadamis Basin, Libya. *Sedimentary Geology*, 329, p.62-80.
- Klitzsch, E., 1968. Outline of the Geology of Libya. p. 71-78, Petroleum Exploration Society of Libya, 10<sup>th</sup> Annual Field Conference. Tripoli, Libya.
- Lelubre, M., 1946. *Le Tibesti Septentrional. Esquisse Morphologique et Structurale*. CR Acad Sci. Coloniales, Paris, p.337-357.
- Massa, D. and Moreau-Benoit, A., 1976. *Essai de Synthèse Stratigraphique et Palynologique Du Système Dévonien En Lybie Occidentale*. Revue de l'Institut Français Du Pétrole, 31 (2), p.287-334.
- Miah, M.I., 2014. Porosity Assessment of Gas Reservoir Using Wireline Log Data: A Case Study of Bokabil Formation, Bangladesh. *Procedia Engineering*, 90, p.663-668.
- Mikbel, S.R., 1979. Structural and Configuration Map of the Basement of East and Central Libya. *Neues Jahrbuch für Geologie und Paläontologie - Abhandlungen*, Band 158 Heft 2, p.209-220. DOI: 10.1127/njgpa/158/1979/209
- Minh, C.C., Greg, G., Ramamoorthy, R., and McGeoch, S., 2001. Sonic-Magnetic Resonance Method: A Sourceless Porosity Evaluation in Gas-Bearing Reservoirs. *SPE Reservoir Evaluation and Engineering*, 4 (03), p.209-220. DOI: 10.2118/72180-PA.
- Osman, W., Mohamed, K., Ahmed, E., and Hisham, S., 2021. Petrophysical Evaluation of Sandstone Gas Reservoir Using Integrated Well Logs and Core Data for the Lower Cretaceous Kharita Formation, Western Desert, Egypt. *Journal of Petroleum Exploration and Production Technology*, 11 (10), p.3723-3746.
- Pickett, G.R., 1973. Pattern Recognition as a Means of Formation Evaluation. *The Log Analyst*, 14 (04).
- Quintero, L.F. and Bassiouni, Z., 1998. Porosity Determination in Gas-Bearing Formations. P. SPE-39774-MS in *SPE Permian Basin Oil and Gas Recovery Conference*. SPE.
- Rahuma, K.M. and Ghawar, B.M., 2019. Calculation and Comparison of Water Saturation in Carbonate Formation by Different Methods. *The International Journal of Engineering & Information Technology (IJEIT)*, 5 (2), p.151-154. DOI: 10.36602/ijeit.v5i2.320
- Schlumberger, L.I.C., 2009. *Log Interpretation Charts*. p.202-224. Houston, Texas: Schlumberger Limited.
- Serra, O. and Serra, L., 2003. *Well Logging and Geology*. France, 448p.
- Serra, O. and Abbott, H.T., 1982. The Contribution of Logging Data to Sedimentology and Stratigraphy. *Society of Petroleum Engineers Journal*, 22 (01), p.117-131.
- Serra, O., Baldwin, J., and Quirein, J., 1980. Theory, Interpretation, and Practical Applications of Natural Gamma Ray Spectroscopy. P. SPWLA-1980, *SPWLA annual logging symposium*. SPWLA.
- Soltan, M.A. and Hrouda, M.S., 2022. The Mediterranean and North African Conference and Exhibition (MEDiNA), Tunis, Tunisia, 12-14 September 2022. p.1-4, *Integrated Geophysical, Geological and Petrophysical data to Study the Middle Devonian Aouinet Ouenine F3 Sand Reservoir in ALWafa Field Ghadames Basin, North-West Libya*. Tunis: AAPG Data pages.
- Wang, Z., Nie, X., Zhang, C. Wang, M., Zhao, J., and Jin.L., 2022. Lithology Classification and Porosity Estimation of Tight Gas Reservoirs with Well Logs Based on an Equivalent Multi-Component Model. *Frontiers in Earth Science*, 10, 850023. DOI: 10.3389/feart.2022.850023
- Wyllie, M.R.J., Gregory, A.R., and Gardner, G.H.F., 1958. An Experimental Investigation of Factors Affecting Elastic Wave Velocities in Porous Media. *Geophysics*, 23 (3), p.459-493. DOI: 10.1190/1.1438493.